

SUREL+: Moving from Walks to Sets for Scalable Subgraph-based Graph Representation Learning

Haoteng Yin[†], Muhan Zhang[‡], Jianguo Wang[†], Pan Li^{†§}

[†]Department of Computer Science, Purdue University [‡]Institute for Artificial Intelligence, Peking University

[§]School of Electrical and Computer Engineering, Georgia Institute of Technology

[†]{yinht, csjgwang, panli}@purdue.edu [‡]muhan@pku.edu.cn

ABSTRACT

Subgraph-based graph representation learning (SGRL) has recently emerged as a powerful tool in many prediction tasks on graphs due to its advantages in model expressiveness and generalization ability. Most previous SGRL models face computational issues associated with the high cost of subgraph extraction for each training or test query. Recently, SUREL was proposed to accelerate SGRL, which samples random walks offline and joins these walks online as a proxy of subgraphs for representation learning. Thanks to the reusability of sampled walks across different queries, SUREL achieves state-of-the-art performance in terms of scalability and prediction accuracy. However, SUREL still suffers from high computational overhead caused by node redundancy in sampled walks. In this work, we propose a novel framework SUREL+ that upgrades SUREL by using node sets instead of walks to represent subgraphs. This set-based representation avoids repeated nodes by definition, but node sets can be irregular in size. To address this issue, we design a customized sparse data structure to efficiently store and index node sets, and provide a specialized operator to join them in parallel batches. SUREL+ is modularized to support multiple types of set samplers, structural features, and neural encoders to complement the structure information loss after the reduction from walks to sets. Extensive experiments have been performed to validate SUREL+ in the prediction tasks of links, relation types, and higher-order patterns. SUREL+ achieves 3-11× speedups of SUREL while maintaining comparable or even better prediction performance; compared to other SGRL baselines, SUREL+ achieves ~20× speedups and significantly improves the prediction accuracy.

PVLDB Reference Format:

Haoteng Yin[†], Muhan Zhang[‡], Jianguo Wang[†], Pan Li^{†§}. SUREL+: Moving from Walks to Sets for Scalable Subgraph-based Graph Representation Learning. PVLDB, 16(11): 2939-2948, 2023.

doi:10.14778/3611479.3611499

PVLDB Artifact Availability:

The source code, data, and/or other artifacts have been made available at https://github.com/Graph-COM/SUREL_Plus.

This work is licensed under the Creative Commons BY-NC-ND 4.0 International License. Visit <https://creativecommons.org/licenses/by-nc-nd/4.0/> to view a copy of this license. For any use beyond those covered by this license, obtain permission by emailing info@vldb.org. Copyright is held by the owner/author(s). Publication rights licensed to the VLDB Endowment.

Proceedings of the VLDB Endowment, Vol. 16, No. 11 ISSN 2150-8097.
doi:10.14778/3611479.3611499

1 INTRODUCTION

Graphs are widely used to model interactions in natural sciences and relationships in social life [21, 24]. Graph-structured data in the real world are highly irregular and often large-scale. To solve inference tasks on graphs, graph representation learning (GRL) that studies quantitative representations of graph-structured data has attracted much attention [16, 17, 47]. Recently, subgraph-based GRL (SGRL) has become an important research direction for researchers studying GRL algorithms and systems, as it achieves far better prediction performance than other approaches in many GRL tasks, especially those involving a set of nodes. Given a set of nodes of interest, namely a queried node set, SGRL models such as SEAL [52, 54], GraIL [40], and SubGNN [1] first extract a subgraph around the queried node set (called query-induced subgraph), and then use neural networks to encode extracted subgraphs for prediction. Extensive work shows that SGRL models are more robust [50] and more expressive [5, 13]; while canonical graph neural networks (GNNs) including GCN [23] and GraphSAGE [15] usually fail to make accurate predictions, due to their limited expressive power [9, 14, 54], incapability of capturing intra-node distance information [28, 38], and improper entanglement between receptive field size and model depth [19, 49, 50]. An example in Fig. 1 illustrates how SGRL works for link prediction and demonstrates its advantages over GNNs. Here, canonical GNNs generate and aggregate node-wise representations to predict links, which would map structurally symmetric nodes into the same representation and lead to the ambiguity issue [48, 54]. So far, the advantages of SGRL methods have been proved in many applications, such as link and relation prediction [40, 52, 54], higher-order pattern prediction [30, 33], temporal network modeling [46], recommender systems [53], anomaly detection [1, 6], graph meta-learning [19], subgraph matching [29, 31], and molecular/protein research in life sciences [45].

Albeit with multiple benefits of its algorithm, SGRL methods currently face two major computational challenges: (1) **Query Dependency**. A subgraph must be extracted for each queried node set, which is not reusable across different queries, and cannot be preprocessed if the query is unknown; (2) **Irregularity**. The extracted subgraphs are irregularly sized, resulting in poor batch processing and load-balancing performance. As shown in Fig. 3 (a), subgraph extraction in SEAL [52, 54] is prohibitively slow to be deployed in practice. This inspired recent work on dedicated hardware acceleration for subgraph extraction [11, 36]. However, how to fundamentally improve the scalability and efficiency of SGRL methods remains largely unexplored.

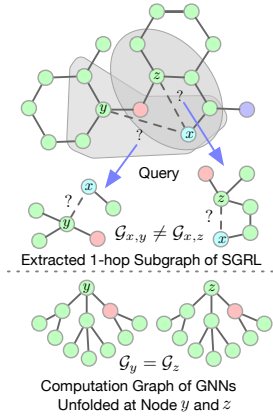


Figure 1: GNNs cannot correctly predict whether x is more likely linked with y or z : without distinct features, y and z have the same node representations. The representations based on one-hop neighbors (query-induced subgraph) are more expressive in distinguishing these two node pairs.

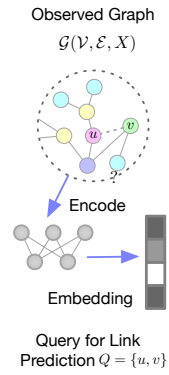


Figure 2: Overview of SUREL+: a side-by-side comparison with previous SGRL models. For a query, SGRL first prepares the input subgraph paired with structural features, which are then fed into a neural encoder to obtain embeddings for prediction. SUREL+ samples node sets as input, while SEAL [52, 54] extracts induced subgraphs and SUREL [49] samples walks. To compensate for structure loss by reducing subgraphs to node sets, SUREL+ provides various types of set samplers, structure encoders, and set neural encoders. To better serve set-based representations, SUREL+ designs a customized sparse data structure SpG to store sampled node sets with fast access, and supports their online joining in parallel via a sparse join operator SpJoin.

	SEAL	SUREL	SUREL+ → Modular Design	
Input Format	1-hop ego-network Query-level G_Q	set of 3-step walks Node-level W_u	reduced node set Node-level S_u	Set Sampler Walk-based, PPR-based Offline
Structural Features	Labeling Trick	Relative Position Encoding (RPE)	Landing Probabilities, Shortest Path Distance, PPR scores	Structure Encoder Offline
Subgraph Encoder	Graph Neural Encoder: GNNs	Sequence Neural Encoder: RNNs	Set Neural Encoder: Mean, Attention, LSTM	Online
Storage	PyG Objects	Associative Array	SpG Objects	Offline
Online Joining	N/A	Multithread Aligned Walk Joining	Multithread Sparse Set Joining SpJoin Operator	Online

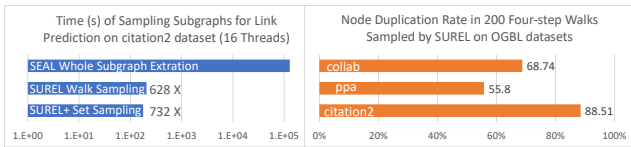


Figure 3: (a) Subgraph extraction in SEAL [52, 54] has much higher complexity than other simplified form samplers. The size of induced subgraphs is irregular, growing exponentially with the number of extracted hops [8, 50]. (b) Breaking subgraphs into reusable walks reduces complexity but faces the issue of heavy node duplicates.

SUREL [49] is the state-of-the-art (SOTA) framework that applies algorithm and system co-design to implement SGRL. It employs the join of node-level sampled walks to represent query-specific subgraphs. Specifically, SUREL treats each node as a seed and runs multiple random walks from the seed on the graph offline. Given a queried node set, SUREL online joins and encodes the sampled walks for all queried nodes for prediction. The join operation builds the connection between sampled walks of queried nodes so that their joint walks can function as the query-induced subgraph. To compensate for the structure loss by representing subgraphs in walks, a structural feature termed relative position encoding (RPE) is adopted to record the position of each distinct node in sampled walks relative to the seed. The RPE is pre-computed offline and attached to sampled walks before being fed into neural networks (NNs) to make predictions. In SUREL, sampled walks from one seed can be reused for multiple queries whenever that seed node is involved. SUREL significantly improves the scalability of SGRL by this walk-sharing mechanism and benefits from the regularity of walks, enabling highly parallel walk sampling and online joining through a dedicated system design. However, SUREL still faces several inherent drawbacks of the walk-based representation, namely high node redundancy in sampled walks (over 55% duplication, see Fig. 3 (b)). This further raises the following issues: (1) **extra space** for hosting walks and positional encoding in memory, (2) **extra time** for operations on repeated nodes in subsequent routines of

walk joining and NN-based encoding, and (3) **high workload** of data transfer between CPU and GPU.

In this work, we upgrade SUREL and develop a novel framework SUREL+ that again benefits from algorithm-system co-design. The core concept of SUREL+ is simple: instead of using walks to represent subgraphs, we now employ node sets, thereby obviating node duplication. However, this new idea based on node sets introduces several algorithm and system design difficulties. From an algorithmic perspective, as explored in this study, the transition from induced subgraphs to walks and then to node sets results in a considerable loss of structural information. Therefore, the first priority is to develop a method that can compensate for structural losses while maintaining performance. On the system side, SUREL [49] utilizes walks, which can be easily stored and processed in an aligned format by controlling the length and number of sampled walks. In contrast, node sets are irregular in size, creating difficulties for efficient storage and fast access. To sum up, how to coordinate the designs of both sides constitutes the primary challenge of this work.

SUREL+ tackles the above challenges throughout its entire pipeline. To avoid node duplication in walk sampling, SUREL+ only keeps unique nodes from each seed node’s sampled neighborhood during preprocessing. To compensate for structure information loss, SUREL+ incorporates various types of set samplers and structure encoders to preserve local structures: *set samplers* employ different graph metrics to measure node importance and determine sampling rules; *structure encoders* support landing probabilities of random walks [27], shortest path distances, and personalized PageRank scores [20], covering most of the structural features used by previous SGRL models [28, 40, 49, 52, 54]. Furthermore, SUREL+ designs a customized sparse data structure, namely SpG, which can efficiently store sampled node sets and achieve fast access. During training and inference, SUREL+ implements a sparse operator SpJoin to perform join operations on the sampled node sets and their associated structural features of all queried nodes, acting as the query-induced subgraph for prediction. In addition, to capture diverse levels of

interactions between node and structural features, SUREL+ supports multiple *set neural encoders*, such as multi-linear perception (MLP) with mean pooling, set attention [41] and LSTM [15] that ensure sufficient expressive power and consistent performance across various types of SGRL tasks.

Overall, our contributions can be summarized as follows:

- Algorithm: SUREL+ is a novel SGRL framework (*open source*), that utilizes reusable node sets and associates them with various types of structural features to represent query-induced subgraphs via online joining. Adopting sets in SUREL+ greatly reduces memory and computation costs without degrading prediction performance compared with the SOTA baselines.
- System: SUREL+ designs a customized sparse data structure SpG and a sparse join operator SpJoin to support efficient storage and processing of node sets, which achieves much better efficiency and scalability than previous SGRL methods.
- We conduct extensive experiments on 9 real-world graphs, with millions/billions of nodes/edges, and demonstrate the advantages of SUREL+ in link/relation-type/motif prediction tasks. SUREL+ is 3-11× faster than the current SOTA SGRL method SUREL while maintaining comparable or even better prediction accuracy. SUREL+ also achieves ~20× speedups with substantial accuracy improvements over other SGRL baselines.

2 PRELIMINARIES

2.1 Notations and Relevant Definitions in SGRL

Let $\mathcal{G}(\mathcal{V}, \mathcal{E}, X)$ be an attributed graph with node set $\mathcal{V} = \{1, 2, \dots, n\}$ and edge set \mathcal{E} , where $X \in \mathbb{R}^{n \times d}$ denotes node attributes with d -dimension. A query $Q \subset \mathcal{V}$ is a node set of interest for a certain type of task. We denote the subgraph induced by query Q as \mathcal{G}_Q and the node-induced subgraph as \mathcal{G}_u , where induced subgraphs are typically within a small number of hops.

Definition 2.1 (Subgraph-based Graph Representation Learning (SGRL)). Given a query Q of node set over graph \mathcal{G} , SGRL aims to learn a representation of the query-induced subgraph \mathcal{G}_Q to make prediction $f(\mathcal{G}_Q)$. (\cdot) is usually a neural network. SGRL tasks come with some labeled queries $\{(Q_i, y_i)\}_{i=1}^L$ for supervision (positive samples) and other unlabeled queries $\{Q_i\}_{i=L+1}^{L+N}$ for inference.

Examples of SGRL Tasks *Link prediction* seeks to estimate the likelihood of a link between two nodes in a given graph, where a query Q corresponds to a node pair. It can be further generalized to predict links with types over heterogeneous graphs [40] or to predict blood vessels [34] and chemical bonds [21] in domain-specific graphs. Tasks beyond pairwise relations are named *higher-order pattern prediction*, where a query Q consists of three or more nodes. In this work, we consider that given partially observed pairwise relations among queried nodes in Q , whether these queried nodes will establish certain full higher-order relation of interest [30, 39].

Review of SGRL Methods The current SGRL pipeline mainly has three parts, as shown in the *Algorithm Design* section of Fig. 2: subgraph preparation, structural feature construction, and neural encoder to obtain subgraph embeddings. Classical SGRL models often group query-dependent parts together (e.g., SEAL [52, 54] couples subgraph extraction with labeling trick [54]), and then

apply neural encoder on extracted subgraphs with attached structural features for prediction. However, such coupling is expensive and makes the computed intermediate results not reusable across queries, which motivates recent SGRL methods to decouple them. SUREL [49] substitutes explicit subgraph extraction with the online joining of multiple walks pre-sampled offline associated with position encoding defined on sampled walks as structural features. Sampled walks and positional encoding are node-level and can be reused to serve multiple queries, which greatly improves efficiency. Lastly, neural networks are applied to encode and aggregate the embedding of joint walks for prediction.

2.2 Related Works

Scalable SGRL Design. Recent works on SGRL models have primarily focused on efficient subgraph extraction. Various techniques have been proposed, including PPR-based [4, 50] and random walk-based [49] subgraph samplers, node neighborhood sampling through CUDA kernel (DGL, [11]) and tensor operations (PyG, [36]). Some frameworks have customized data structures to better support subgraph operations and gain higher throughput, such as associative arrays in SUREL [49], temporal-CSR in TGL [55], and GPU-orientated dictionary in NAT [32]. To achieve scalable modeling design, GDGNN [25] utilizes node representations along the geodesic path between queried nodes for prediction, partially decoupling structural feature construction from subgraph extraction. BUDDY [7] employs subgraph sketches to avoid explicitly constructing subgraphs for link prediction. However, these works either focus on specific aspects of the SGRL scalability issue, namely extraction, storage, and feature construction bottlenecks, or are limited to one type of SGRL tasks. In contrast, SUREL+ provides a comprehensive co-design approach in scalable sampling, efficient storage, and expressive modeling, offering a general subgraph-based framework for scalable SGRL.

3 THE FRAMEWORK OF SUREL+

This section introduces SUREL+, whose key concept is to offline sample node sets around seed nodes in the graph, which can be joined online as a proxy of query-induced subgraph for representation learning. This approach keeps only distinct nodes in the sampled set for reuse in different queries, effectively addressing memory and computation concerns of node duplication in existing walk-based representations adopted by SUREL [49]. SUREL+ features a modular design that supports various set samplers and structure encoders, and different set neural encoders can be paired with diverse structural features to compensate for the structure information loss after reducing subgraphs to node sets. Furthermore, SUREL+ introduces a customized sparse data structure SpG and an arithmetic operator SpJoin to store node sets and perform their online joins efficiently. Fig. 2 summarizes and compares SUREL+ and current SGRL models. The following subsections describe these modules in detail.

3.1 Set Samplers and Structure Encoders

SUREL+ uses set samplers to sample a set of nodes from the neighborhood of each seed node in the graph and calls structure encoders

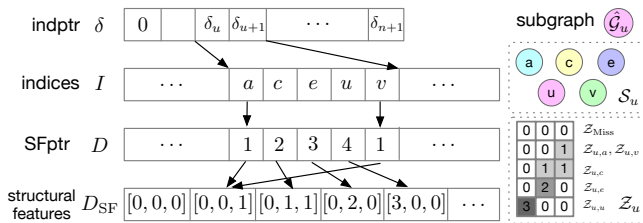


Figure 4: Node set \mathcal{S}_u and its associated structural features \mathcal{Z}_u stored in SpG. It contains three arrays to store the node set size, its elements, and associated structural features (with optional two-level indexing). Here, D_{SF} shows the landing counts of nodes at different steps in sampled walks as an example, which can be normalized later to landing probabilities as structural features.

to construct structural features. Both operations are executed offline: the former is primarily for computational benefits, while the latter is to offset the structure loss of node sets reducing from subgraphs (adopted by SEAL [52, 54]) or walks (adopted by SUREL [49]). Conceptually, SUREL+ represents the node-induced subgraph \mathcal{G}_u via a combination of (1) a node set \mathcal{S}_u comprising unique nodes sampled from the neighborhood of node u and (2) the associated structural features \mathcal{Z}_u reflects the position of sampled nodes in \mathcal{G}_u .

Set Samplers Two types of set samplers are adopted. The first type, named *Walk-based Sampler*, is to sample short-step random walks and eliminate repeated nodes during sampling. The second type, named *Metric-based Sampler*, is based on more principled graph metrics that measure the proximity between neighboring nodes and the seed node, such as personalized PageRank (PPR) scores [20] or short path distances. Specifically, the walk-based sampler runs M -many m -step random walks, starting from each seed u in parallel on the graph \mathcal{G} , and then puts only distinct nodes in sampled walks into set \mathcal{S}_u . The metric-based sampler, taking PPR-based [4] as an example, first runs the push-flow algorithm [2] to obtain an approximation of the PPR vector for each seed u , and then selects the top- K nodes with the highest PPR scores into set \mathcal{S}_u . Mathematically, PPR scores are convergent landing probabilities of seeded random walks that reach infinite steps. Therefore, these two samplers complement each other by leveraging either more local or global structures of the graph. We use hyper-parameters M, m to control random walks, and K to control metric-based samplers, which are all set as some constants in practice. The complexity of the above offline sampling procedures is $O(|\mathcal{V}|)$.

Structure Encoders The structure encoder is to construct structural features $\mathcal{Z}_{u,x} \in \mathbb{R}^k$ for each node x in the sampled node set \mathcal{S}_u . These features prove to be crucial for inference tasks on graphs involving multiple nodes [54] and can be conceptually understood as anchoring sampled node x in the seed u 's neighborhood. One possible choice is landing probabilities of random walk [27, 28, 49]: each element $\mathcal{Z}_{u,x}[i]$ stores the counts of node x landed at step i of all walks rooted at the seed node u divided by the total number of walks performed by the sampler. Landing probabilities (LPs) can be computed along with walk sampling. Another option is the shortest path distance (SPD) between x and u [28, 52, 54], which records their relative distance in terms of reachability. PPR scores [20] is another popular structural feature and can be naturally obtained by running a PPR-based sampler. Later, we denote the collection of structural features for all nodes in \mathcal{S}_u as $\mathcal{Z}_u = \{\mathcal{Z}_{u,x} | x \in \mathcal{S}_u\}$.

Table 1: Complexity comparison of GRL models. Suppose using $O(|\mathcal{E}|)$ -many queries, SGRs use partial edges ($q \ll |\mathcal{E}|$) for training. S and K denote the average size of extracted subgraphs and sampled node sets, respectively. L is the number of layers. d and k are respective dimensions of node and structural features. Assume d is fixed for all layers. Both SUREL and SUREL+ use the walk-based sampler for M -many m -step walks. c is the number of distinct k -dim structural features. δ_{n+1} is the size sum of all node sets.

Methods	GNN [23]	SEAL [52, 54]	SUREL [49]	SUREL+
Structure	$O(\mathcal{V} + \mathcal{E})$	$O(S \mathcal{E})$	$O(mM \mathcal{V})$	$O(\delta_{n+1})$
Feature	$O(d \mathcal{V})$	$O(kS \mathcal{E})$	$O(\delta_{n+1} * k)$	$O(\delta_{n+1} + c * k)$
Time	$O(\mathcal{E} Ld + \mathcal{E} Ld^2)$	$O(qS^Ld^2)$	$O(qmMd^2)$	$O(qKd^2)$

3.2 Set-based Storage - SpG

Node-set-based representations have advantages in terms of flexibility and compactness. However, the uneven sizes of sampled node sets pose great challenges to their storage and fast access. Note that these node sets are frequently visited in subsequent online phases for inference. To overcome these obstacles, SUREL+ designs a customized compressed sparse row (CSR) format called SpG, which reorganizes the storage of node sets and their structural features in a memory-efficient manner, as depicted in Fig. 4. Specifically, the node set \mathcal{S}_u and its structural features \mathcal{Z}_u are stored as a row of SpG, denoted as $\text{SpG}[u, :]$. Multiple node sets and their associated structural features are consolidated into three contiguous arrays:

- **indptr $\delta \in \mathbb{Z}^{n+1}$** , an integer array tracks the starting index of each stored node set (row). It records the cumulative sum of the sizes of all node sets $\mathcal{S}_u, \forall u \in \mathcal{V}$, e.g., $\delta_{u+1} = \delta_u + |\mathcal{S}_u|$, where $|\mathcal{S}_u|$ represents the size of the set \mathcal{S}_u . The total number of sampled nodes stored in SpG is δ_{n+1} ;
- **indices $I \in \mathbb{Z}^{\delta_{n+1}}$** , a coalesce array of all node sets $\mathcal{S}_u, \forall u \in \mathcal{V}$. The segment $I[\delta_u : \delta_{u+1}]$ corresponds to the indices of sampled nodes of \mathcal{S}_u stored in sorted order. This ordering is particularly useful for speeding up the join operation discussed in Sec. 3.3.
- **SFptr $D \in \mathbb{R}^{\delta_{n+1}}$** , a pointer array contains the indices of the structural features \mathcal{Z}_u stored in the array D_{SF} . The purpose of D_{SF} is to eliminate duplicate structural features that typically reside in GPU memory. This secondary index can further reduce memory needs, especially when using LPs/SPDs that are likely to have many repeated values, but it is not necessary when using PPR scores since they tend to have distinct values.

Regarding the cost of SpG, indptr array is of size $|\mathcal{V}| + 1$, and the size of both indices and SFptr arrays is δ_{n+1} . The compressed encoding array D_{SF} , has a size of $c * k$, where c is the number of distinct structural features and k denotes feature dimension. The overall complexity of this data structure is $O(|\mathcal{V}| + \delta_{n+1} + c * k)$.

Comparison with Other Methods Table 1 summarizes the space and time complexity comparison of GRL methods. By adopting the walk-based sampler (sampling M -many m -step walks), δ_{n+1} amounts to around one-fifth space used by SUREL of $O(mM|\mathcal{V}|)$, while the metric-based sampler (sampling top- K PPR scores) results in $\delta_{n+1} = K|\mathcal{V}|$ and $K < mM$ in general. Both values are substantially lower than $O(S|\mathcal{E}|)$ used by SEAL, where S is the average size of sampled subgraphs. For hosting structural features, SUREL+ employs the secondary index SFptr D and retains only distinct structural features in D_{SF} to further reduce the memory footprint.

In practice, c typically remains independent of $|\mathcal{V}|$. Equipped with SpG, SUREL+ is capable of handling industry-level graph data.

3.3 Joining Node Sets via Sparse Operations

The goal of joining node sets is to connect queried nodes and construct query-induced subgraphs from pre-sampled node sets to make predictions for SGRL queries. For a given query Q , we merge relevant node sets $S_u, \forall u \in Q$ into $\mathcal{S}_Q = \bigcup_{u \in Q} S_u$ and join their node-level structural features \mathcal{Z}_u to the query level. In essence, query-level structural features \mathcal{Z}_Q serve as an anchor that indicates the position of node $x \in \mathcal{S}_Q$ within the query-induced subgraph \mathcal{G}_Q . Specifically, for a node x in \mathcal{S}_Q , the query-level structural features $\mathcal{Z}_{Q,x}$ are obtained by joining its node-level structural features $\mathcal{Z}_{u,x}$ for all queried node u in Q as

$$\mathcal{Z}_{Q,x} = \parallel_{u \in Q} \mathcal{Z}_{u,x} = [\dots \mathcal{Z}_{u,x} \dots] \in \mathbb{R}^{|\mathcal{Q}| \times k}, \quad (1)$$

where \parallel denotes concatenation. In cases where $\mathcal{Z}_{u,x}$ does not exist as node $x \notin S_u$ while $u \in Q$, it is set to all zeros. For instance, in Fig. 5, node b is in S_v but not in S_u , hence $\mathcal{Z}_{u,b}$ is set to zero. \mathcal{Z}_Q is a collection of $\mathcal{Z}_{Q,x}, \forall x \in \mathcal{S}_Q$. Together, \mathcal{S}_Q and \mathcal{Z}_Q function as the query-induced subgraph \mathcal{G}_Q , which is fed into the neural encoder later to obtain embeddings for prediction.

The JOIN operator in databases is used to merge tables and establish connections. Concatenation in Eq. (1) requires matching among different node sets with varying sizes and arbitrary node orders, where an outer JOIN is well-suited for this task. In this case, the JOIN operator returns associated values based on the node index (specified common field) from target sets, regardless of its existence. To obtain $\mathcal{Z}_{Q,x}$, node sets $\{S_u\}_{u \in Q}$ are treated as tables: if the index of a node x matches one of the node indices in S_u for all u in Q , then the associated structural features $\mathcal{Z}_{u,x}$ are appended; otherwise, the field is filled with zeros. However, iterating over all S_u 's to retrieve $\mathcal{Z}_{u,x}$ for each node $x \in \mathcal{S}_Q$ is highly inefficient, as its complexity can be $O(|Q| * |\mathcal{S}_Q|^2)$ per query. This becomes even more challenging when performing these operations for massive queries with varying sizes of S_u and \mathcal{S}_Q .

To tackle this issue, we design an efficient arithmetic operator SpJoin to perform joins on sparse data objects of SpG in parallel. This operator reduces the time complexity to $O(|Q| * |\mathcal{S}_Q|)$ per query by taking advantage of node indices of S_u stored in SpG are unique and in sorted order. The following demonstrates the use of SpJoin for a query $Q = \{u, v\}$.

Sparse Join Operator The operator SpJoin performs an outer JOIN on the sampled node sets from seeds u and v of query Q stored in SpG as $\text{SpG}[u, :]$ and $\text{SpG}[v, :]$ through

$$\text{SpJoin}(\text{SpG}[u, :], \text{SpG}[v, :]) = \text{SpAdd}(\text{mask}, \text{SpG}[u, :]) - 1 \parallel \text{SpAdd}(\text{mask}, \text{SpG}[v, :]) - 1$$

where $\text{mask} = \text{bool}(\text{SpAdd}(\text{SpG}[u, :], \text{SpG}[v, :]))$.

As illustrated in Fig. 5, SpJoin consists of three steps:

- (1) It utilizes sparse arithmetic operations from SciPy [42]: SpAdd performs an element-wise addition ($X \oplus Y$) of the non-zero elements in X and Y ; the resulting values are converted to binary via the `bool` operator and saved in the mask, which corresponds to node indices of the set \mathcal{S}_Q .

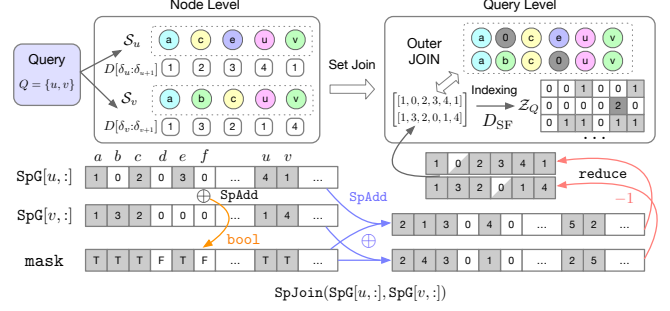


Figure 5: An illustration of joining structural features from node-level to query-level (Eq. (1)) via the SpJoin operator on node sets stored in SpG. Note that SpG objects do not physically carry 0 as above shown in $\text{SpG}[u, :]$ and $\text{SpG}[v, :]$. Only non-zero elements in grey blocks are stored in SpG and performed arithmetic operations by SpJoin. The half-grey blocks correspond to added missing values.

- (2) `SpAdd` are applied between mask and each $\text{SpG}[u, :], \forall u \in Q$ following by the reduction `-1`, which explicitly adds missing values (all zeros at default) to structural features $\mathcal{Z}_{u,x}$ for all x if $x \notin S_u$ while $x \in S_v$, for some $v \in Q \setminus \{u\}$.
- (3) When the secondary index SFptr D is used, the results of SpJoin are pointers saved in SFptr, which can be used to gather the values of structural features \mathcal{Z}_Q from the array D_{SF} .

Multithreading is employed to leverage the single program multiple data pattern in sparse operations of SpJoin. Since the processing time of each query linearly depends on the size of \mathcal{S}_Q , we further divide queries of each training batch into groups with nearly balanced sums of $|\mathcal{S}_Q|$'s, and assign one thread process a group to mitigate potential delays caused by uneven workloads.

Comparison with SUREL [49] SUREL adopts hash-based join operators to build query-level structural features, but its overall computation and memory cost is much higher compared to SUREL+. This is due to the presence of numerous repeated nodes in walks (over half as Fig. 3 (b) shown). The set-based input of SUREL+ substantially reduces the workload of transferring data from CPU to GPU and also requires fewer per-node operations on GPU to process transmitted \mathcal{Z}_Q 's. As Table 1 shows, SUREL+ reduces time complexity from $O(mM)$ to $O(K)$, where $K < mM$ is the average size of sampled node sets. These advantages ultimately enable SUREL+ to achieve superior efficiency and scalability.

3.4 Set Neural Encoders

After joining sampled node sets for each query Q , the resulting $(\mathcal{S}_Q, \mathcal{Z}_Q)$ acts as the query-induced subgraph \mathcal{G}_Q and then is fed into neural encoders for prediction. The mini-batch training procedure of multiple queries is summarized in Algorithm 1. Next, we introduce neural encoders supported by SUREL+.

The adopted neural encoders are simple. For each $(\mathcal{S}_Q, \mathcal{Z}_Q)$,

$$h_Q = \text{AGGR}(\{\text{enc}(\mathcal{Z}_{Q,x}) | x \in \mathcal{S}_Q\}) \in \mathbb{R}^d. \quad (2)$$

Here, $\text{enc}(\cdot)$ encodes query-level structural features $\mathcal{Z}_{Q,x}$ using a multi-linear perception. If node attributes are present, they can be appended to the structural features as $\mathcal{Z}_{Q,u} \parallel X_u$. AGGR is used to aggregate the encoded features, which can be any neural encoders applied on sets such as mean/sum/max pooling or set transformers.

Algorithm 1: The mini-batch training pipeline of SUREL+

Input: Given a graph $\mathcal{G}(\mathcal{V}, \mathcal{E}, X)$, a group of queries $\{(Q, y_Q)\}$ for training, batch size B , a set SAMPLER, a structure ENCODER, and a set AGGR

Output: A neural network for encoding subgraphs $enc(\cdot)$

- 1 Preprocessing: SAMPLER and ENCODER $\rightarrow (S_u, Z_u)$ for all $u \in \mathcal{V}$; convert and save (S_u, Z_u) 's as SpG objects.
 - 2 **for** each mini-batch $Q_B = \{\dots, Q, \dots\}$ **do**
 - 3 Generate negative training queries (if not given) $\{\tilde{Q}_B\}$ by random sampling and put them into Q_B ;
 - 4 Call SpJoin operator to perform joining on SpG objects $\{(S_u, Z_u) | u \in Q\}$ for all queries $Q \in Q_B$ in parallel;
 - 5 Encode the joined results (S_Q, Z_Q) as proxy of subgraphs via Eq. (2) with specified AGGR and get the prediction \hat{y}_Q from readout h_Q by multithreads;
 - 6 Backward propagation based on the loss $\mathcal{L}(\hat{y}_Q, y_Q)$.
 - 7 **end**
-

Currently, SUREL+ supports the implementations of AGGR in mean pooling, LSTM [15], and attention [41]. Note that the LSTM applies random permutations to the elements in the set before encoding them as a sequence; while the attention first computes soft attention scores based on the output of $enc(\cdot)$ for each set element and then performs attention-score-weighted pooling. Sec. 4.4 empirically demonstrates that the choice of AGGR has non-trivial effects on prediction performance. Lastly, a fully connected layer takes the readout h_Q as input to make the final prediction \hat{y}_Q . In our experiments, all SGRL tasks are formulated as binary classification, and thus Binary Cross Entropy is used as the loss function \mathcal{L} .

4 EVALUATION

In this section, we aim to evaluate the following questions:

- Regarding space and time complexity, how much improvement can SUREL+ achieve by adopting sets instead of walks compared to the SOTA SGRL framework SUREL?
- Can SUREL+ provide comparable prediction performance to all baselines using or not using SGRL methods?
- How sensitive is SUREL+ to different choices of set samplers, structure encoders, and set neural encoders?
- How do sparse storage SpG and parallelism in SpJoin operator benefit the overall performance of SUREL+?

4.1 Experiment Setup

Extensive experiments have been performed to evaluate SUREL+ using homogeneous, heterogeneous, and higher-order homogeneous graphs on three types of tasks: link prediction, relation type prediction, and higher-order pattern prediction. A homogeneous graph is a graph that does not include node/link types, while a heterogeneous graph includes various node/link types. Higher-order graphs are hypergraphs in our setting that contain hyperedges connecting two or more nodes.

Datasets Table 2 summarizes the statistics of datasets used to benchmark SGRL methods. Five datasets are selected from the Open Graph Benchmark (OGB, [18]) for link and relation type prediction, including social networks of citation - citation2 and

Table 2: Summary Statistics for Evaluation Datasets.

Dataset	Type	#Nodes	#Edges	Split(%)
criteo-click	Homo./Bipartite	Campaign: 675 User: 6,142,256	16,468,027	97/1.5/1.5
twitter-2010	Homo./Social.	41,652,230	1,468,364,884	99.98/0.01/0.01
citation2	Homo./Social.	2,927,963	30,561,187	98/1/1
collab	Homo./Social.	235,868	1,285,465	92/4/4
ppa	Homo./Bio.	576,289	30,326,273	70/20/10
vessel	Homo./Bio.	3,538,495	5,345,897	80/10/10
ogb-mag	Hetero.	(P): 736,389 (A): 1,134,649	P-A: 7,145,660 P-P: 5,416,271	99/0.5/0.5
tags-math	Higher.	1,629	projected: 91,685 hyperedges: 822,059	60/20/20
DBLP-coauthor	Higher.	1,924,991	projected: 7,904,336 hyperedges: 3,700,067	60/20/20

collaboration - collab; biological network of protein interaction - ppa and blood vessels - vessel; and one heterogeneous academic network ogb-mag, which contains node types of paper (P), author (A) and their extracted relations. The vessel dataset is a large (>3M nodes), sparse, biological graph recently constructed from mouse brains [34] and has unique significance for examining GRL in scientific discovery. The structure of vessels illustrates the spatial organization of the brain's microvasculature, which can be used for early detection of neurological disorders, e.g. Alzheimer's and stroke. Two hypergraph datasets collected by [3] are used for higher-order pattern prediction: DBLP-coauthor is a temporal hypergraph, where each hyperedge denotes a time-stamped paper connecting all its authors. tags-math contains sets of tags applied to questions on the website math.stackexchange.com, represented as hyperedges. For higher-order pattern prediction tasks, the number of hyperedges is the main computation bottleneck, in which one may connect more than two nodes. Two industry-level graphs, criteo-click with 16.5M records of online banner ads clicking [12] and twitter-2010 with 1.5B following relations of users [26] are used to examine the model scalability for real-world applications.

Settings For link prediction, OGB's standard data split is used to isolate validation and test links from the input graph. For prediction tasks of relation type and higher-order pattern, the same procedure to prepare graph data is adopted as in [49]: the relations of paper-author (P-A, "written by") and paper-paper (P-P, "cited by") are selected; higher-order queries in hypergraph datasets are node triplets, where the goal is to predict whether it will foster in a hyperedge given two of them have observed pairwise connections; to learn the representation on hypergraphs, we project hyperedges into cliques and treat the projection results as ordinary graphs. All experiments are run 10 times independently, and we report the mean performance and standard deviation.

Baselines We consider two classes of baselines. *Canonical GNNs*: GCN [23], GraphSAGE [15], GraphSAINT [51] and their variants with the prefix 'H*' that are directly applied for heterogeneous graphs with node types and for hypergraphs through clique expansion. R-GCN [37] performs relational message passing on heterogeneous graphs; *Scalable GNNs*: and Cluster-GCN [10]; SGRL models: SEAL [52, 54], GDGNN [25], and SUREL [49]. SEAL adopts online subgraph sampling due to its intractable space needs for offline subgraph extraction. Fig. 3 (a) compares the time cost for subgraph sampling across different SGRL methods. We use all baselines' official implementations with hyperparameter tuning to match their reported results.

Table 3: Prediction Performance for Links, Relation Types and Higher-Order Patterns: the best (bold) and the second best (underlined).

Models	citation2	click MRR (%)	twitter	collab Hits@50 (%)	ppa Hits@100 (%)	vessel ROC-AUC	Models	MAG(P-A)	MAG(P-P)	tags-math MRR (%)	DBLP-coauthor
GCN	84.74±0.21	5.31±0.17	OOM	44.75±1.07	18.67±1.32	43.53±9.61	H*GCN	39.43±0.29	57.43±0.30	51.64±0.27	37.95±2.59
GraphSAINT	79.85±0.40	2.86±0.63	4.12±0.73	53.12±0.52	3.83±1.33	47.14±6.83	H*SAGE	25.35±1.49	60.54±1.60	54.68±2.03	22.91±0.94
GDGNN	86.96±0.28	13.30±0.45	<u>49.86±0.39</u>	54.74±0.48	45.92±2.14	75.84±0.08	R-GCN	37.10±1.05	56.82±4.71	-	-
SEAL	87.67±0.32	OOM	OOM	<u>63.64±0.71</u>	48.80±3.16	80.50±0.21	SUREL	<u>45.33±2.94</u>	82.47±0.26	<u>71.86±2.15</u>	<u>97.66±2.89</u>
SUREL	89.74±0.18	<u>40.39±0.61</u>	OOM	63.34±0.52	<u>53.23±1.03</u>	86.16±0.39	SUREL+	58.81±0.42	<u>80.45±0.13</u>	77.73±0.16	99.83±0.02
SUREL+	<u>88.90±0.06</u>	60.87±0.15	55.67±0.67	64.10±1.06	54.32±0.44	<u>85.73±0.88</u>	/	/	/	/	/

Table 4: Breakdown of Runtime, Memory Consumption for Different Models on Prediction of Link, Relation Type, and Higher-order Pattern. The column Train records the runtime per 10K queries.

Models	Runtime (s)					Memory (GB)					Runtime (s)					Memory (GB)				
	Prep.	Train	Inf.	RAM	SDRAM	Prep.	Train	Inf.	RAM	SDRAM	Prep.	Train	Inf.	RAM	SDRAM	Prep.	Train	Inf.	RAM	SDRAM
Dataset	criteo-click					twitter-2010					citation2					ppa				
GCN	3	0.085	8	3.1	62.74	-	-	-	-	OOM	17	21.74	105	9.3	36.84	2	0.026	1.2	4.6	11.35
GraphSAINT	1	0.012	20	13.1	8.79	111	0.009	920	253	76.60	151	1.79	107	9.6	9.78	10	0.003	1.5	4.9	23.06
GDGNN	215	1.43	2,928	16.2	23.77	1204	1.84	9,744	188	79.34	338	2.26	5,460	40.6	16.96	127	1.77	902	21.1	10.27
SEAL	-	-	-	OOM	-	-	-	-	OOM	-	46	3.52	24,626	35.4	5.71	46	10.57	3,988	9.5	12.13
SUREL	2	1.59	2,307	11.7	16.25	-	-	-	OOM	-	151	4.14	6,081	25.1	9.68	31	2.68	1,429	13.6	31.01
SUREL+	22	0.23	502	10.4	11.93	327	0.26	3,779	210	49.44	130	0.35	1,389	16.7	4.75	69	0.72	201	9.8	19.02

Hyperparameters By default, SUREL+ uses the walk-based sampler, the structural encoder LP and the better set neural encoder tuned between mean pooling and attention. SUREL+ adopts a 2-layer MLP as $enc(\cdot)$ in Eq. (2) followed by a 2-layer MLP classifier to map set-aggregated representations for final predictions. Default training hyperparameters: learning rate $lr=1e-3$ with the early stopping of 5 epochs, dropout $p=0.1$, Adam [22] as the optimizer. Analysis of parameters M and m to control the walk-based sampler and K to control the metric-based sampler and selection of structure encoders and set neural encoders are studied in Sec. 4.4.

Evaluation Metrics The evaluation metrics include Hits@P, Mean Reciprocal Rank (MRR), and Area Under Curve (ROC-AUC). Hit@P counts the ratio of positive samples ranked at the top-P place against negative ones. MRR first computes the inverse of the rank of the first correct prediction and then takes the average of obtained reciprocal ranks for a sample of queries. For all datasets adopting MRR, each positive query is paired with 1000 randomly sampled negative test queries, except tags-math using 100 and criteo-click using 650. ROC-AUC follows the standard definition to measure the model’s performance in binary classification.

Environment We use a server with two Intel Xeon Gold 6248R CPUs, 512GB DRAM, and NVIDIA A100 (80GB) GPU. SUREL+ is built on PyTorch 1.12 and PyG 2.2. Set samplers are implemented in C, OpenMP, NumPy, Numba, and uhash, integrated into Python scripts; SpG is customized based on the CSR format of Scipy [42].

4.2 Prediction Accuracy Comparison

Table 3 shows the prediction performance of different methods. SGRL models significantly outperform canonical GNNs on these six link prediction benchmarks, especially on two challenging biological datasets ppa and vessel. Predicting links in biological datasets requires richer structural information that canonical GNNs have limited expressive power to capture. Within SGRL models, SUREL+ achieves comparable performance to SUREL and outperforms SEAL,

which validates the effectiveness of the proposed set-based subgraph representation. For predictions of relation type and higher-order pattern, we observe additional performance gains (+2~13%) from SUREL+ compared to SUREL on three of the four datasets. A large performance gap exists between canonical GNNs and SGRL models, particularly in the higher-order case. This demonstrates the inherent limitations of canonical GNNs to make predictions of complex relations involving multiple nodes.

4.3 Efficiency and Scalability Analysis

Improved Efficiency in Training and Inference. Table 4 compares model runtime and memory usage on the four largest benchmarks. SUREL+ offers a reasonable training time compared with canonical GNNs. It shows clear improvement in inference compared to the current SOTA framework SUREL (3-11× speedups across all datasets) and its predecessor SEAL (~20× speedups). SUREL+ achieves comparable and even lower RAM usage than canonical GNNs. Compared to other SGRL models, it can save up to half of RAM with lower usage of GPU DRAM, since set-based subgraphs eliminate node duplicates and their associated structural features. Tables 1 and 4 analytically and empirically show that the key factor of SUREL+ scaling up to billion-size graphs is its set-based representation with the sparse design, while GCN (full adjacency matrix), SEAL (complex subgraph extraction) and SUREL (dense walks with duplicate nodes) are all out of memory (OOM) on twitter-2010.

Profiling Different Strategies for Offline Processing. Fig. 6a reports the time cost of different samplers with multithreading on citation2. Fig. 6b shows memory consumption to store different types of sampled data (walks in SUREL [49] or sets in SUREL+) and their associated structural features (LPs, SPDs, PPR scores). Compared to SUREL sampler[49], the walk-based sampler in SUREL+ is more scalable and only adds one extra minute for encoding and converting data in SpG format (slash/dash marked in Fig. 6a), while achieving 6.94×, 3.63× and 4.12× memory savings on three OGB

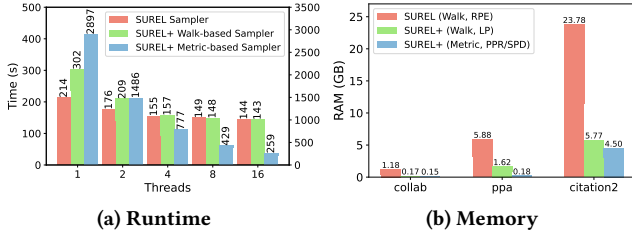


Figure 6: Comparison of Runtime, Memory Consumption across Different Offline Processing Strategies (the walk-based sampler: $m = 4$, $M = 200$, the metric-based sampler: $K = 150$). The areas highlighted break down the total consumption w.r.t. (a) sampling, structure encoding, sparse object construction; (b) structural features, node indices/pointers, and sampled walks (SUREL sampler only).

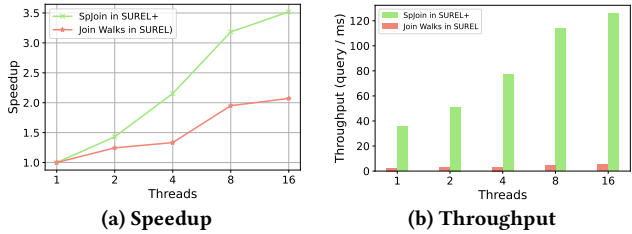


Figure 7: Scaling Performance Comparison of SpJoin in SUREL+ (with average set size $|\bar{S}_u| = 351$) and Join Walks in SUREL (with walk size $m = 4$, $M = 200$) against Different Numbers of Threads.

datasets, respectively. Those memory savings are crucial for model scalability as they reduce the workload of data transfer from CPU to GPU and save GPU operations from encoding duplicated nodes, which dominates the time cost of the online stage and leads to the efficiency improvement of SUREL+ in Table 4. In addition, the metric-based sampler that adopts PPR scores has better scaling performance with more threads. When PPR scores or SPDs are adopted as structural features, SUREL+ further reduces the memory cost, though they often harm prediction performance slightly.

Note that in the above comparison of memory cost, compressed structural features are adopted both in SUREL (locally) and SUREL+ (globally), i.e., the secondary index based on $Sfptr D$ and D_{SF} , which achieve compression of $493\times$, $11318\times$, $19527\times$ on three datasets listed in Fig. 6b, when one adopts LPs as structural features.

Scaling Analysis for SpJoin. Fig. 7 shows the speedups and throughput of the SpJoin operator for constructing query-level structural features via multithreading, where the join operation in SURE for nodes in walks [49] is used for comparison. SUREL employs a hash-based search for walk joins, which has unfavorable memory access patterns and suffers from imbalanced workloads due to inconsistent searching times across threads. SUREL+ gains more benefits from multithreading, thanks to sparse arithmetic operations and batch-wise load balancing used in SpJoin.

4.4 Comparison between Different Set Samplers, Structural Features and Set Neural Encoders

SUREL+ is a modularized framework that supports different set samplers (walk- and metric-based), structural features (LP, SPD, PPR), and set neural encoders AGGR (mean pooling, LSTM, attention).

Table 5: Prediction Performance and Inference Runtime of SUREL+ with Different Combinations of Structure Features (LP, SPD, PPR) and Set Neural Encoders (Mean, LSTM, Attn.). The best and the second best are highlighted in bold and underlined accordingly.

Dataset	PPR+Mean	SPD+Mean	LP+Mean	LP+LSTM	LP+Attention
citation2	78.59 ± 0.38	87.99 ± 1.07	<u>88.55 ± 0.15</u>	88.46 ± 0.34	<u>88.90 ± 0.06</u>
	834	1057s	1389s	3678s	2171s
collab	47.15 ± 0.21	62.11 ± 0.13	<u>64.10 ± 1.06</u>	61.31 ± 1.37	<u>62.85 ± 1.19</u>
	1.4s	<u>1.7s</u>	2.0s	3.5s	2.3s
ppa	13.28 ± 1.20	41.06 ± 1.70	46.41 ± 1.65	<u>54.45 ± 1.35</u>	<u>54.32 ± 0.44</u>
	63s	<u>126s</u>	165s	322s	201s

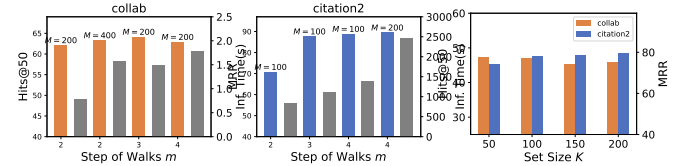


Figure 8: Hyperparameter Analysis of Set Samplers (Prediction Performance v.s. Time Cost). Walk-based: the number M and the step m of walks, LPs as structural features; Metric-based: the set size K , PPR scores as structural features.

Table 5 shows the prediction performance and inference runtime by adopting different combinations of structure encoders and set neural encoders. Landing probabilities (LPs) as structural features perform the best on all three OGB datasets while being the slowest for inference. By recording the landing probabilities over different steps of walks, LPs provide structural information in finer granularity than scalar values of SPDs and PPR scores. The adopted link prediction task might favor more local information held by LPs and SPDs than global information carried by PPR scores. The authors conjecture that other tasks that rely on more global information may favor PPR scores. In comparison, no set neural encoder is always a winner. Attention seems to perform the best on average while slower than mean pooling. LSTM is the slowest. On the two social networks (citation2 and collab), mean pooling can provide comparable prediction results with much fewer parameters. However, prediction on the biological network (ppa) requires more expressive and complicated encoders, where LSTM and attention are favored as they can model more complex interactions between nodes in the joint set S_Q .

Fig. 8 compares prediction results and inference time by using different hyperparameters m , M , and K of set samplers, which heavily affects the coverage of sampled neighborhoods and computation overhead. The performance consistently increases if the walk-based sampler uses a larger M , but is not guaranteed for a larger m (broader exploration). Better coverage with a larger K is usually beneficial for the metric-based sampler over citation2 but not for collab, which is due to different characteristics of these two datasets and is also observed by [49]. In general, small sampling parameters m ($2 \sim 4$), M ($100 \sim 400$) and K ($50 \sim 200$) can yield satisfactory performance with fast inference speed that achieves the trade-off between accuracy and scalability.

5 CONCLUSION

In this work, we propose a novel framework SUREL+ for scalable subgraph-based graph representation learning. SUREL+ avoids

costly query-specific subgraph extraction by decoupling it into sampled node sets with structural features whose join can function as query-induced subgraphs for prediction. SUREL+ benefits from the reusability and compactness of pre-sampled node sets across different queries. Compared to the SOTA SGRL framework SUREL, the set-based representation of SUREL+ substantially reduces space and time complexity by avoiding heavy node duplicates in sampled walks. To handle irregularly sized node sets, SUREL+ designs a customized sparse storage SpG and a sparse join operator SpJoin, providing memory-efficient storage with fast access. In addition, SUREL+ adopts a modular design, enabling users to choose different set samplers, structure encoders, and set neural encoders flexibly based on the nature of their SGRL tasks. Extensive experiments on three types of prediction tasks over nine real-world graph benchmarks show that SUREL+ significantly improves scalability, memory efficiency, and prediction accuracy compared to current SGRL methods and canonical GNNs.

ACKNOWLEDGMENTS

The authors would like to thank Rongzhe Wei and Yanbang Wang for their helpful discussions and valuable feedback. Haoteng Yin and Pan Li are supported by the 2021 JPMorgan Faculty Award, NSF awards OAC-2117997, IIS-2239565.

REFERENCES

- [1] Emily Alsentzer, Samuel Finlayson, Michelle Li, and Marinka Zitnik. 2020. Subgraph neural networks. *Advances in Neural Information Processing Systems* 33 (2020), 8017–8029.
- [2] Reid Andersen, Fan Chung, and Kevin Lang. 2006. Local graph partitioning using pagerank vectors. In *2006 47th Annual IEEE Symposium on Foundations of Computer Science (FOCS'06)*. IEEE, 475–486.
- [3] Austin R Benson, Rediet Abebe, Michael T Schaub, Ali Jadbabaie, and Jon Kleinberg. 2018. Simplicial closure and higher-order link prediction. *Proceedings of the National Academy of Sciences* 115, 48 (2018), E11221–E11230.
- [4] Aleksandar Bojchevski, Johannes Klicpera, Bryan Perozzi, Amol Kapoor, Martin Blais, Benedek Rózemberczki, Michal Lukasik, and Stephan Günnemann. 2020. Scaling graph neural networks with approximate pagerank. In *Proceedings of the 26th ACM SIGKDD International Conference on Knowledge Discovery and Data Mining*. 2464–2473.
- [5] Giorgos Bouritsas, Fabrizio Frasca, Stefanos P Zafeiriou, and Michael Bronstein. 2022. Improving graph neural network expressivity via subgraph isomorphism counting. *IEEE Transactions on Pattern Analysis and Machine Intelligence* (2022).
- [6] Lei Cai, Zhengzhang Chen, Chen Luo, Jiaping Gui, Jingchao Ni, Ding Li, and Haifeng Chen. 2021. Structural temporal graph neural networks for anomaly detection in dynamic graphs. In *Proceedings of the 30th ACM International Conference on Information & Knowledge Management*. 3747–3756.
- [7] Benjamin Paul Chamberlain, Sergey Shirobokov, Emanuele Rossi, Fabrizio Frasca, Thomas Markovich, Nils Hammerla, Michael M Bronstein, and Max Hansmire. 2023. Graph Neural Networks for Link Prediction with Subgraph Sketching. In *International Conference on Learning Representations*.
- [8] Jie Chen, Tengfei Ma, and Cao Xiao. 2018. Fastgcn: fast learning with graph convolutional networks via importance sampling. In *International Conference on Learning Representations*.
- [9] Zhengdao Chen, Lei Chen, Soledad Villar, and Joan Bruna. 2020. Can graph neural networks count substructures? *Advances in Neural Information Processing Systems* 33 (2020), 10383–10395.
- [10] Wei-Lin Chiang, Xuanqing Liu, Si Si, Yang Li, Samy Bengio, and Cho-Jui Hsieh. 2019. Cluster-gcn: An efficient algorithm for training deep and large graph convolutional networks. In *Proceedings of the 25th ACM SIGKDD International Conference on Knowledge Discovery and Data Mining*. 257–266.
- [11] DGL. 2022. 6.7 Using GPU for Neighborhood Sampling – DGL 0.9.1post1 documentation. <https://docs.dgl.ai/guide/minibatch-gpu-sampling.html>
- [12] Eustache Diemert, Julien Meynet, Pierre Galland, and Damien Lefortier. 2017. Attribution modeling increases efficiency of bidding in display advertising. In *Proceedings of the AdKDD and TargetAd Workshop*. ACM, 1–6.
- [13] Fabrizio Frasca, Beatrice Bevilacqua, Michael M Bronstein, and Haggai Maron. 2022. Understanding and Extending Subgraph GNNs by Rethinking Their Symmetries. *Advances in Neural Information Processing Systems* 35 (2022).
- [14] Vikas Garg, Stefanie Jegelka, and Tommi Jaakkola. 2020. Generalization and representational limits of graph neural networks. In *International Conference on Machine Learning*. PMLR, 3419–3430.
- [15] Will Hamilton, Zhitao Ying, and Jure Leskovec. 2017. Inductive representation learning on large graphs. *Advances in Neural Information Processing Systems* 30 (2017), 1025–1035.
- [16] William L Hamilton. 2020. Graph representation learning. *Synthesis Lectures on Artificial Intelligence and Machine Learning* 14, 3 (2020), 1–159.
- [17] William L. Hamilton, Rex Ying, and Jure Leskovec. 2017. Representation Learning on Graphs: Methods and Applications. *IEEE Data Eng. Bull.* 40, 3 (2017), 52–74.
- [18] Weihua Hu, Matthias Fey, Marinka Zitnik, Yuxiao Dong, Hongyu Ren, Bowen Liu, Michele Catasta, and Jure Leskovec. 2020. Open graph benchmark: Datasets for machine learning on graphs. *Advances in Neural Information Processing Systems* 33 (2020), 22118–22133.
- [19] Kexin Huang and Marinka Zitnik. 2020. Graph meta learning via local subgraphs. *Advances in Neural Information Processing Systems* 33 (2020), 5862–5874.
- [20] Glen Jeh and Jennifer Widom. 2003. Scaling personalized web search. In *Proceedings of the 12th International Conference on World Wide Web*. 271–279.
- [21] John Jumper, Richard Evans, Alexander Pritzel, Tim Green, Michael Figurnov, Olaf Ronneberger, Kathryn Tunyasuvunakool, Russ Bates, Augustin Židek, Anna Potapenko, et al. 2021. Highly accurate protein structure prediction with AlphaFold. *Nature* 596, 7873 (2021), 583–589.
- [22] Diederik P. Kingma and Jimmy Ba. 2015. Adam: A method for stochastic optimization. In *International Conference on Learning Representations*.
- [23] Thomas N Kipf and Max Welling. 2017. Semi-supervised classification with graph convolutional networks. In *International Conference on Learning Representations*.
- [24] Daphne Koller, Nir Friedman, Sašo Džeroski, Charles Sutton, Andrew McCallum, Avi Pfeffer, Pieter Abbeel, Ming-Fai Wong, Chris Meek, Jennifer Neville, et al. 2007. *Introduction to statistical relational learning*. MIT press.
- [25] Lecheng Kong, Yixin Chen, and Muhan Zhang. 2022. Geodesic Graph Neural Network for Efficient Graph Representation Learning. *Advances in Neural Information Processing Systems* 35 (2022).
- [26] Haewoon Kwak, Changhyun Lee, Hosung Park, and Sue Moon. 2010. What is Twitter, a social network or a news media?. In *Proceedings of the 19th international conference on World wide web*. 591–600.
- [27] Pan Li, I Chien, and Olgica Milenkovic. 2019. Optimizing generalized pagerank methods for seed-expansion community detection. *Advances in Neural Information Processing Systems* 32 (2019), 11710–11721.
- [28] Pan Li, Yanbang Wang, Hongwei Wang, and Jure Leskovec. 2020. Distance Encoding: Design Provably More Powerful Neural Networks for Graph Representation Learning. *Advances in Neural Information Processing Systems* 33 (2020), 4465–4478.
- [29] Xin Liu, Haojie Pan, Mutian He, Yangqiu Song, Xin Jiang, and Lifeng Shang. 2020. Neural subgraph isomorphism counting. In *Proceedings of the 26th ACM SIGKDD International Conference on Knowledge Discovery and Data Mining*. 1959–1969.
- [30] Yunyu Liu, Jianzhu Ma, and Pan Li. 2022. Neural Predicting Higher-Order Patterns in Temporal Networks. In *Proceedings of the Web Conference 2022*. ACM, 1340–1351.
- [31] Zhaoyu Lou, Jiaxuan You, Chengtao Wen, Arquimedes Canedo, Jure Leskovec, et al. 2020. Neural Subgraph Matching. *arXiv preprint arXiv:2007.03092* (2020).
- [32] Yuhong Luo and Pan Li. 2022. Neighborhood-aware Scalable Temporal Network Representation Learning. *Learning on Graphs Conference* (2022).
- [33] Changping Meng, S Chandra Mouli, Bruno Ribeiro, and Jennifer Neville. 2018. Subgraph pattern neural networks for high-order graph evolution prediction. In *Proceedings of the AAAI Conference on Artificial Intelligence*, Vol. 32.
- [34] Johannes C Paetzold, Julian McGinnis, Suprosanna Shit, Ivan Ezhov, Paul Büschl, Chinmay Prabhakar, Anjany Sekuboyina, Mihail Todorov, Georgios Kaissis, Ali Ertürk, et al. 2021. Whole Brain Vessel Graphs: A Dataset and Benchmark for Graph Learning and Neuroscience. In *Thirty-fifth Conference on Neural Information Processing Systems Datasets and Benchmarks Track*.
- [35] Jingshu Peng, Zhao Chen, Yingxia Shao, Yanyan Shen, Lei Chen, and Jiannong Cao. 2022. Sancus: staleness-aware communication-avoiding full-graph decentralized training in large-scale graph neural networks. *Proceedings of the VLDB Endowment* 15, 9 (2022), 1937–1950.
- [36] PyG. 2022. Accelerating PyG on NVIDIA GPUs. <https://www.pyg.org/ns-newsarticle-accelerating-pyg-on-nvidia-gpus>
- [37] Michael Schlichtkrull, Thomas N Kipf, Peter Bloem, Rianne Van Den Berg, Ivan Titov, and Max Welling. 2018. Modeling relational data with graph convolutional networks. In *European semantic web conference*. Springer, 593–607.
- [38] Balasubramaniam Srinivasan and Bruno Ribeiro. 2020. On the equivalence between positional node embeddings and structural graph representations. In *International Conference on Learning Representations*.
- [39] Balasubramaniam Srinivasan, Da Zheng, and George Karypis. 2021. Learning over Families of Sets-Hypergraph Representation Learning for Higher Order Tasks. In *Proceedings of the 2021 SIAM International Conference on Data Mining (SDM)*. SIAM, 756–764.

- [40] Komal Teru, Etienne Denis, and Will Hamilton. 2020. Inductive relation prediction by subgraph reasoning. In *International Conference on Machine Learning*. PMLR, 9448–9457.
- [41] Petar Veličković, Guillem Cucurull, Arantxa Casanova, Adriana Romero, Pietro Lio, and Yoshua Bengio. 2018. Graph attention networks. In *International Conference on Learning Representations*.
- [42] Pauli Virtanen, Ralf Gommers, Travis E. Oliphant, Matt Haberland, Tyler Reddy, David Cournapeau, Evgeni Burovski, Pearu Peterson, Warren Weckesser, Jonathan Bright, Stéfan J. van der Walt, Matthew Brett, Joshua Wilson, K. Jarrod Millman, Nikolay Mayorov, Andrew R. J. Nelson, Eric Jones, Robert Kern, Eric Larson, C J Carey, İlhan Polat, Yu Feng, Eric W. Moore, Jake VanderPlas, Denis Laxalde, Josef Perktold, Robert Cimrman, Ian Henriksen, E. A. Quintero, Charles R. Harris, Anne M. Archibald, Antônio H. Ribeiro, Fabian Pedregosa, Paul van Mulbregt, and SciPy 1.0 Contributors. 2020. SciPy 1.0: Fundamental Algorithms for Scientific Computing in Python. *Nature Methods* 17 (2020), 261–272.
- [43] Cheng Wan, Youjie Li, Ang Li, Nam Sung Kim, and Yingyan Lin. 2022. BNS-GCN: Efficient full-graph training of graph convolutional networks with partition-parallelism and random boundary node sampling. *Proceedings of Machine Learning and Systems* 4, 673–693.
- [44] Cheng Wan, Youjie Li, Cameron R Wolfe, Anastasios Kyriklidis, Nam Sung Kim, and Yingyan Lin. 2022. Pipegc: Efficient full-graph training of graph convolutional networks with pipelined feature communication. In *International Conference on Learning Representations*.
- [45] Xiyuan Wang and Muhan Zhang. 2021. GLASS: GNN with Labeling Tricks for Subgraph Representation Learning. In *International Conference on Learning Representations*.
- [46] Yanbang Wang, Yen-Yu Chang, Yunyu Liu, Jure Leskovec, and Pan Li. 2021. Inductive Representation Learning in Temporal Networks via Causal Anonymous Walks. In *International Conference on Learning Representations*.
- [47] Lingfei Wu, Peng Cui, Jian Pei, Liang Zhao, and Xiaojie Guo. 2022. Graph neural networks: foundation, frontiers and applications. In *Proceedings of the 28th ACM SIGKDD Conference on Knowledge Discovery and Data Mining*. 4840–4841.
- [48] Keyulu Xu, Weihua Hu, Jure Leskovec, and Stefanie Jegelka. 2019. How Powerful are Graph Neural Networks?. In *International Conference on Learning Representations*.
- [49] Haoteng Yin, Muhan Zhang, Yanbang Wang, Jianguo Wang, and Pan Li. 2022. Algorithm and System Co-design for Efficient Subgraph-based Graph Representation Learning. *Proceedings of the VLDB Endowment* 15, 11 (2022), 2788–2796.
- [50] Hanqing Zeng, Muhan Zhang, Yinglong Xia, Ajitesh Srivastava, Andrey Malevich, Rajgopal Kannan, Viktor Prasanna, Long Jin, and Ren Chen. 2021. Decoupling the depth and scope of graph neural networks. *Advances in Neural Information Processing Systems* 34 (2021), 19665–19679.
- [51] Hanqing Zeng, Hongkuan Zhou, Ajitesh Srivastava, Rajgopal Kannan, and Viktor Prasanna. 2020. Graphsaint: Graph sampling based inductive learning method. In *International Conference on Learning Representations*.
- [52] Muhan Zhang and Yixin Chen. 2018. Link prediction based on graph neural networks. *Advances in Neural Information Processing Systems* 31 (2018), 5165–5175.
- [53] Muhan Zhang and Yixin Chen. 2020. Inductive Matrix Completion Based on Graph Neural Networks. In *International Conference on Learning Representations*.
- [54] Muhan Zhang, Pan Li, Yinglong Xia, Kai Wang, and Long Jin. 2021. Labeling Trick: A Theory of Using Graph Neural Networks for Multi-Node Representation Learning. *Advances in Neural Information Processing Systems* 34 (2021), 9061–9073.
- [55] Hongkuan Zhou, Da Zheng, Israt Nisa, Vasileios Ioannidis, Xiang Song, and George Karypis. 2022. TGL: A General Framework for Temporal GNN Training on Billion-Scale Graphs. *Proceedings of the VLDB Endowment* 15, 8 (2022), 1572–1580.

A NOTATIONS

Frequently used symbols are summarized in Table 6.

B MORE DETAILS

B.1 Other Related Works

Scalable GNN Design. GNNs are the most widely used tools for graph representation learning nowadays, although they face certain challenges when directly applied to subgraph-based methods. To address the scalability of GNNs, current studies focus on improving graph subsampling and mini-batch training techniques [10, 51]. However, graph subsampling used in GNNs fundamentally differs

Table 6: Summary of Frequently Used Notations.

Symbol	Meaning
Q	a query (set of nodes), i.e. $Q = \{u, v, w\}$
\mathcal{Q}	a set of queries, i.e. $Q \in \mathcal{Q}$
\mathcal{G}_u	a subgraph induced by node u
\mathcal{G}_Q	a subgraph induced by query Q
\mathcal{S}_u	a set of unique nodes sampled from the neighborhood of the seed node u
$\mathcal{Z}_{u,x}$	structural features of node x regarding the seed node u (all zeros if $x \notin \mathcal{S}_u$)
\mathcal{Z}_u	collection of structural features for all nodes in \mathcal{S}_u as $\mathcal{Z}_u = \{\mathcal{Z}_{u,x} x \in \mathcal{S}_u\}$
\parallel	the concatenation that joins node-level structural features, i.e. join $\mathcal{Z}_{\cdot,x}$ for a query $Q = \{u, v, w\}$ as $[\mathcal{Z}_{u,x}, \mathcal{Z}_{v,x}, \mathcal{Z}_{w,x}]$.
$\mathcal{Z}_{Q,x}$	query-level structural features for node x regarding the query Q , $\mathcal{Z}_{Q,x} = \parallel_{u \in Q} \mathcal{Z}_{u,x}$

from subgraph extractions in SGRL. The goal of subsampling is to handle GPU memory overflow during full-batch training of GNN models. For SGRL, subgraphs sampled around a query serve as features for making predictions. Consequently, the scaling techniques developed for GNNs cannot be directly applied to SGRL. Another direction is to deploy distributed GNN systems for industry-level graphs. Unfortunately, these specialized techniques, including pipelining [44], partitioned parallelism [43], and update with staleness [35] do not address the main bottleneck of subgraph extraction for SGRL methods.

B.2 Model Design

Benefits of Subgraph-based Graph Representation Learning
 First, subgraph-based representation is versatile for different types of tasks, especially when queries of certain tasks involving multiple nodes and relations, e.g. existence of a link, property of a motif, development of higher-order patterns; while canonical GNNs are limited to handle such polyadic dynamics via node-wise representations [38, 45] (also refers to the example in Fig. 1). Second, subgraph-based models are more expressive by pairing with structural features to obtain most expressive structural node representations [5, 28, 38, 45]. However, canonical GNNs cannot capture intra-distance information and joint relations over multiple nodes, which are critical to distinguishing nodes in structural symmetry and making predictions over them. Lastly, subgraph-based methods decouple the model depth from the receptive field since extracted subgraphs are localized to certain hops: when adding more layers for non-linearity, it does not contaminate embedding with irrelevant nodes or get over-smooth as canonical GNNs do. This results in a more robust representation and is particularly beneficial for modeling relations beyond singleton.

B.3 Datasets

The full statistics of benchmark datasets are summarized in Table 7. OGB datasets¹ are selected to benchmark our proposed framework and other baselines. It contains large-scale graphs (millions

¹https://ogb.stanford.edu/docs/dataset_overview/

Table 7: Summary Statistics and Experimental Setup for Evaluation Datasets.

Dataset	Type	#Nodes	#Edges	Avg. Node Deg.	Density	Split Ratio	Split Type	Metric
criteo-click	Homo./Bipartite	Campaign(C): 675 User(U): 6,142,256	16,468,027	2.68	N/A	97/1.5/1.5	Time	MRR
twitter-2010	Homo./Social.	41,652,230	1,468,364,884	35.25	0.00017%	99.98/0.01/0.01	Random	MRR
citation2	Homo./Social.	2,927,963	30,561,187	20.7	0.00036%	98/1/1	Time	MRR
collab	Homo./Social.	235,868	1,285,465	8.2	0.0046%	92/4/4	Time	Hits@50
ppa	Homo./Bio.	576,289	30,326,273	73.7	0.018%	70/20/10	Throughput	Hits@100
vessel	Homo./Bio.	3,538,495	5,345,897	3.02	0.000085%	80/10/10	Random	AUC-ROC
ogb-mag	Hetero.	Paper(P): 736,389 Author(A): 1,134,649	P-A: 7,145,660 P-P: 5,416,271	21.7	N/A	99/0.5/0.5	Time	MRR
tags-math	Higher.	1,629	91,685 (projected) 822,059 (hyperedges)	N/A	N/A	60/20/20	Time	MRR
DBLP-coauthor	Higher.	1,924,991	7,904,336 (projected) 3,700,067 (hyperedges)	N/A	N/A	60/20/20	Time	MRR

Table 8: [Extended] Breakdown of Runtime, Memory Consumption for Different Models on Prediction of Link, Relation Type, and Higher-order Pattern. The column Train records the runtime per 10K queries.

Models	Runtime (s)		Memory (GB)		Runtime (s)		Memory (GB)		Runtime (s)		Memory (GB)		Runtime (s)		Memory (GB)					
	Prep.	Train	Inf.	RAM	SDRAM	Prep.	Train	Inf.	RAM	SDRAM	Prep.	Train	Inf.	RAM	SDRAM	Prep.	Train	Inf.	RAM	SDRAM
Dataset	citation2				ppa				collab				vessel							
GCN	17	21.74	105	9.3	36.84	2	0.026	1.2	4.6	11.35	2	0.005	0.05	2.5	5.50	5	0.076	0.3	2.8	36.98
GraphSAINT	151	1.79	107	9.6	9.78	10	0.003	1.5	4.9	23.06	1	0.004	0.08	2.5	8.11	5	0.008	15	6.9	10.21
GDGNN	338	2.26	5,460	40.6	16.96	127	1.77	902	21.1	10.27	14	0.74	15	4.3	1.08	25	0.85	84	7.2	8.03
SEAL	46	3.52	24,626	35.4	5.71	46	10.57	3,988	9.5	12.13	5	4.05	37	4.0	6.20	6	10.69	998	6.2	2.46
SUREL	151	4.14	6,081	25.1	9.68	31	2.68	1,429	13.6	31.01	1	2.13	17	3.4	9.86	5	1.57	32	5.8	5.18
SUREL+	130	0.35	1,389	16.7	4.75	69	0.72	201	9.8	19.02	7	0.27	2	2.8	3.37	3	0.31	3	3.3	1.25
Dataset	MAG(P-A)				MAG(P-P)				tags-math				DBLP-coauthor							
H*GCN	3	0.03	9	5.0	21.56	4	0.03	13	5.5	21.66	2	0.004	1.3	2.4	3.10	-	0.58	95	8.0	25.80
H*SAGE	3	0.03	10	5.0	20.29	4	0.03	13	5.5	20.28	1	0.003	1.3	2.4	3.10	-	0.32	77	7.5	24.70
R-GCN	1	0.52	5	5.3	26.34	1	0.52	4	5.1	31.41	-	-	-	-	-	-	-	-	-	-
SUREL	10	3.20	1,998	7.3	7.18	15	0.99	1924	8.1	16.66	-	2.13	341	3.0	5.95	11	1.29	949	9.7	7.79
SUREL+	58	0.33	101	7.2	2.95	77	0.13	168	8.1	13.49	1	0.67	116	2.4	5.70	8	0.24	315	3.8	3.16

of nodes/edges) for real-world applications (i.e., academic and biological networks) and provides standard, open-sourced evaluation metrics and tools. Note that, `vessel` is a newly added benchmark of a biological graph, with $> 3M$ nodes and sparse vessel structures extracted from the whole mouse brain [34], where nodes represent bifurcation points, and edges represent the blood vessels. Each node is associated with features of its physical location in the coordinate space (x, y, z) . The introduction of `vessel` provides a unique opportunity to examine graph representation learning (GRL) approaches in neuroscience, especially in scaling subgraph-based GRL methods to handle sparse and spatial graphs with millions of nodes and edges for scientific discovery.

`criteo-click` contains a sample of 30 days of Criteo live traffic data, each corresponding to one impression (a banner) displayed to a user and whether it is clicked [12]. Each record has 9 contextual features that are aggregated into a 270-dimensional edge feature. There are 675 unique campaign banners and 6.1M users, consisting of a bipartite graph of 16.5M edges: 97% is used for training, and the rest is evenly split for validation and testing based on temporal orders. The task is to predict which campaign the user is most likely to click among 651 candidates. `twitter-2010` is an industry-level social network with 1.5B following relations of users [26]. An edge (i, j) of this network indicates that user i is followed by user j . 1% of Twitter users who follow 10 to 1000 accounts are

randomly sampled for evaluation. The task is to recommend which account they will most likely follow among 1001 candidates. The OGB formatted files of these two datasets are accessible via Box at <https://purdue.box.com/v/SGRL-LSC-dataset>.

B.4 Baselines

For link prediction and relation type prediction, baseline models are selected based on their scalability and prediction performance from the current OGB leaderboard². All models listed on the leaderboard are publicly accessible. We adopt their reported numbers on the leaderboard with verification. For the rest of the baselines, we benchmark these models using their official implementations with tuned hyperparameters as listed below.

- **Canonical GCNN**: a graph auto-encoder model that uses graph convolution layers to learn node representations, including GCN [23], GraphSAGE [15], and their more scalable variants by employing graph subsampling, such as Cluster-GCN [10], GraphSAINT [51].
- **R-GCN³** [37]: a relational GCN that models heterogeneous graphs with different types of node/link.
- **SEAL⁴** [52]: apply GCN on exact query-induced subgraphs with double radius node labeling to obtain subgraph-level readout

²https://ogb.stanford.edu/docs/leader_linkprop/

³https://github.com/pyg-team/pytorch_geometric/blob/master/examples

⁴https://github.com/facebookresearch/SEAL_OGB

for link prediction. SEAL shows great empirical performance on multiple graph machine learning benchmarks and promotes the deployment of subgraph-based models for scientific discovery. The implementation we tested is specialized for OGB datasets provided in [54].

- **GDGNN**⁵ [25]: a model aggregates node representations generated by GNNs along geodesic paths between nodes in a query to speedup subgraph-based methods.
- **SUREL**⁶ [49]: a walk-based computation framework to accelerate subgraph-based methods, where subgraphs are decomposed to pre-sampled walks and then are joined online to substitute the query-induced subgraph for prediction. SUREL achieves state-of-the-art scalability and prediction accuracy on SGRL tasks by adopting walk-based representation.

All canonical GNN baselines⁷ come with three GCNConv/SAGEConv layers of 256 hidden dimensions, and a tuned dropout ratio in $\{0, 0.5\}$ for full-batch training. Canonical GNN models aggregate all node embeddings involved in a query as the representations of links/hyperedges, which are later fed into an MLP classifier for final prediction. In addition, all GNN models need to use full training data (edges/triplets) to generate robust node representations. The hypergraph datasets do not come with raw node features, thus GNN baselines here use randomly initialized features as input for training along with other model parameters. R-GCN uses RGCNConv layers that support message passing with multiple relation types between different types of nodes, where the edge types (relations) are used as input beside node features.

Subgraph-based models only use partial edges/triplets for training. For SEAL, 1-hop enclosing subgraphs are extracted online during the training and inference. Then, it applies three GCN layers of 32 hidden dimensions plus a sort pooling and several 1D convolution layers to generate a readout of the target subgraph for prediction. SUREL consists of a 2-layer MLP for relative position encoding (RPE) and a 2-layer RNN to encode joined walks attached with RPEs to obtain the readout of query-level subgraphs. The hidden dimension of both networks is set to 64. The obtained embeddings of joined walks are aggregated and fed into a 2-layer MLP classifier to make predictions. GDGNN employs GINLayer as its backbone to obtain node embeddings. The horizontal geodesic representation is used for predictions, which finds the shortest path between two nodes in a query and aggregates node representations generated by GNNs along the found geodesic path. The max search distance for geodesic is the same as the number of GNN layers. For `collab`, `ppa`, `citation2` and `vessel`, the threshold of distance is set to 4, 4, 3, and 2, respectively. The hidden dimension of all fully connected layers is set to 32.

C ARCHITECTURE AND HYPERPARAMETER

SUREL+ uses a 2-layer MLP with ReLU activation for encoding structural features and supports three set neural encoders, including mean pooling, LSTM, and attention. LSTM interprets elements to be aggregated in a set as a sequence [15]; attention first calculates soft attention scores for elements in a set and then performs

Table 9: Hyperparameters Used for Benchmark SUREL+.

Dataset	#steps m	#walks M	#negative samples k	Structural Feature	Set Neural Encoder
<code>criteo-click</code>	4	200	10	LP	Mean
<code>twitter-2010</code>	4	100	25	LP	Mean
<code>citation2</code>	4	100	10	LP	Mean
<code>collab</code>	3	200	10	LP	Mean
<code>ppa</code>	4	200	20	LP	Attn.
<code>vessel</code>	2	50	5	LP	Mean
MAG (P-A)	3	200	10	LP	Mean
MAG (P-P)	4	100	10	LP	Mean
<code>tags-math</code>	4	200	10	LP	Mean
<code>DBLP-coauthor</code>	3	100	10	LP	Mean

attention-score-weighted average pooling. The hidden dimension of all parameterized layers is set to 96. Lastly, hidden representations of joined node sets are fed into a 2-layer MLP classifier for final predictions.

For the implementation of set samplers, the walk-based sampler builds on the sampling function from SubGAcc⁸ library developed by the authors, which also provides the support for efficient structural feature compression and index remapping. The metric-based sampler is adopted from fast PPR approximation in [4].

We follow the inductive setting for link and relation prediction: only partial samples will be used for training. Over the training graph, we randomly select 5% links as positive training queries, each paired with k -many negative samples ($k = 10$ by default). We mask these links and use the remaining 95% links to compute each node’s structural features in the split training set via structure encoder. For `vessel`, as the input graph is very sparse, we first sort the nodes in training set by their degree and then randomly pick 5% nodes to obtain edges of their 2-hop induced subgraphs for training and the rest reserved for structural feature construction. For higher-order pattern prediction, we use the given graph before timestamp t to sample node sets and encode their structural features. The model parameters are optimized by triplets provided in the training set. No node features are used in SUREL+, except for `vessel` where normalized physical locations of each node are attached after its structural features and contextual features of `click` are attached.

The extended version of Table 4 is provided in Table 8 for the comparison on the rest of the datasets. The results reported in Table 3 and the profiling of SUREL+ in Tables 4, 8 are obtained through the combination of hyperparameters listed in Table 9. The dropout rate on `vessel` is set to $p=0.2$. The metric-based sampler is adopted to obtain the results of using PPR and SPD as structural features in Table 5. Its sampling size K is set to 50, 50 and 150 for `collab`, `ppa`, `citation2`, respectively. The walk-based sampler is used for the results of LP as structural features, whose sampling parameters are listed in Table 9. The rest of the hyperparameters remain the same as reported in Sec. 4.1. The SUREL+ framework including SubGAcc library is open-source and free for academic use under the BSD-2-Clause license.

⁵<https://github.com/woodcutter1998/gdgnn>

⁶<https://github.com/Graph-COM/SUREL>

⁷<https://github.com/snap-stanford/ogb/tree/master/examples/linkpropped>

⁸https://github.com/VeritasYin/subg_acc